

A new combined analysis of elastic and charge exchange $KN(\overline{KN})$ scatterings in the Regge realm

Byung-Geel Yu*

Research Institute of Basic Science, Korea Aerospace University, Koyang, 10540, Korea

Kook-Jin Kong†

(Dated: September 13, 2019)

The Regge features of elastic $K^\pm N \rightarrow K^\pm N$, and charge exchange $K^- p \rightarrow \overline{K}^0 n$ and $K^+ n \rightarrow K^0 p$ reactions are described by using a combined analysis of all these channels at high momenta. Based on the meson exchanges in the t -channel with their decays to $K\overline{K}$ pair allowed, the exchanges of $\rho(775) + \omega(782)$ are excluded in contrast to existing model calculations and the present work follows a new scheme for the meson exchanges $a_0(980) + \phi(1020) + f_2(1275) + a_2(1320)$ reggeized for the forward elastic scattering amplitude together with Pomeron. The charge exchange reactions are described by $a_0(980) + a_2(1320)$ exchanges in the t -channel. Dominance of the isoscalar f_2 and Pomeron exchanges beyond $P_{\text{Lab}} \approx 3 \text{ GeV}/c$ is shown in the elastic process. Both the isovector a_0 and a_2 exchanges in charge exchange reactions play the respective roles in the low and high momentum region. Differential and total cross sections are presented to compare with existing data. Discussion is given to the polarization of $K^- p \rightarrow K^- p$ at $P_{\text{Lab}} = 10 \text{ GeV}/c$ and $K^- p \rightarrow \overline{K}^0 n$ at $P_{\text{Lab}} = 8 \text{ GeV}/c$.

PACS numbers: 11.55.Jy, 13.75.Jz, 13.85.Dz, 14.20.Pt

I. INTRODUCTION

Meson-baryon scatterings are the most fundamental reactions to understand strong interaction purely on hadronic bases. Among these reactions, KN and \overline{KN} scatterings are interesting, because they could offer a testing ground for the formation of exotic baryons in the K^+N reaction [1–4] as well as the kaonic bound state through the K^-N channel coupling [5, 6]. Above the region, $P_{\text{Lab}} \geq 3 \text{ GeV}/c$, of course, the t -channel meson exchange becomes dominant and in the elastic process, in particular, the Pomeron exchange is expected to yield a nonresonant diffraction toward high momenta up to hundreds of GeV/c [7].

To date, however, in comparison to an effort to understand the reaction mechanism at low momentum [6, 8], the description of such a high momentum aspect of KN (\overline{KN}) scattering is less challenged, since after the early stage of the Regge theory with the residue fitted to empirical data [9]. It has been a convention that the exchanges of ρ and ω mesons are included to give contributions based on the combined fitting procedure to πN and KN data with their coupling strengths from the $SU(3)$ symmetry [10–14]. On the other hand, from their decay modes to $K\overline{K}$ which are forbidden kinematically, these lighter vector mesons are highly off-shell and, thus, their coupling constants should also be highly model-dependent, if participating in the reaction. This is true for lighter meson exchanges in the NN scattering. In practice, the former reaction proceeds via the exchanged

meson decaying to $K\overline{K}$ in the t -channel, whereas the latter case undergoes exchange of strong force between two nucleon lines by the exchange of virtual mesons with hadron form factors. In these respect, the meson-baryon scattering could be treated differently from the baryon-baryon scattering, when the virtual mesons should decay to the on shell $K\overline{K}$ pair, as are the cases of ρ and ω .

Further, we recall that in the total (reaction) cross sections of $K^\pm p \rightarrow K^\pm p$ [7] the roles of ρ and ω exchanges are unique to distinguish between K^+p and K^-p cross sections at high momenta, though far away from their on-shell propagations. However, such a conspicuous difference is not observed in experimental data between elastic $K^\pm p$ scatterings. Rather, they are coincident to each other, in contrast to the case of total cross section. Thus, we are led to consider a single Pomeron exchange without $\rho + \omega$ exchanges for the elastic $K^\pm p$ phenomena at high momenta. This issue will be pointed out in the Appendix with a demonstration for the inconsistency of the $\rho + \omega$ exchanges with the elastic $K^\pm p$ cross sections.

In hadron models which are based on the on-shell Born amplitudes such as the standard pole model, or its Reggeized version, it is hard to employ these lighter vector mesons without either a large uncertainty in their coupling strengths or a model dependence due to the cut-off form factors. Therefore, with a question about how the theory without $\rho + \omega$ exchanges could work on the elastic KN (\overline{KN}) scattering, it is worth investigating the reaction based on a new scheme of the t -channel meson exchange with those that are decaying to $K\overline{K}$ as reported in the Particle Data Group (PDG).

In our previous work [15] we investigated forward scattering of πN elastic and charge exchange processes in the Regge model where the relativistic Born terms for the t -channel mesons were reggeized with the interaction

* bgyu@kau.ac.kr

† kong@kau.ac.kr

Lagrangians and coupling constants sharing with those widely accepted in other hadron reactions. The diffractive features of elastic reactions up to hundreds of GeV/c pion momentum were well described by the Pomeron exchange that we constructed from the quark-Pomeron coupling picture. In this work we extend the framework of Ref. [15] to apply for KN ($\bar{K}N$) scattering via four elastic channels,

$$K^+p \rightarrow K^+p, \quad (1)$$

$$K^-p \rightarrow K^-p, \quad (2)$$

$$K^+n \rightarrow K^+n, \quad (3)$$

$$K^-n \rightarrow K^-n, \quad (4)$$

and two charge exchange processes

$$K^+n \rightarrow K^0p, \quad (5)$$

$$K^-p \rightarrow \bar{K}^0n, \quad (6)$$

respectively.

The paper is organized as follows. In Sec. II we begin with construction of the Reggeized meson exchange for elastic and charge exchange KN ($\bar{K}N$) scatterings, excluding $\rho + \omega$ exchanges as discussed in the introduction. The t -channel meson exchanges are applied to elastic KN ($\bar{K}N$) scattering to describe the reaction at the Regge realm. Numerical consequences are compared to experimental data on total and differential cross sections at high momentum region. Section III is devoted to an analysis of the KN ($\bar{K}N$) charge exchange reaction to reproduce experimental data of total and differential cross sections and beam polarization asymmetry. Summary and discussion follow in Sec. IV to evaluate physical meaning of our findings in the present approach. In the Appendix we present a numerical evidence for elastic KN ($\bar{K}N$) cross section with and without $\rho + \omega$ exchanges to support the present approach.

II. ELASTIC KN ($\bar{K}N$) SCATTERING IN THE REGGEIZED MODEL

In the kaon elastic scattering process on nucleon target,

$$K^\pm(k) + N(p) \rightarrow K^\pm(q) + N(p'), \quad (7)$$

the incoming and outgoing kaon momenta are denoted by k and q , and the initial and final nucleon momenta by p and p' , respectively. Then, conservation of four-momentum requires $k + p = q + p'$, and $s = (k + p)^2$, $t = (q - k)^2$, and $u = (p' - k)^2$ are invariant Mandelstam variables corresponding to each channel.

Within the present framework where the relativistic Born amplitudes are employed to be reggeized, the exchanges of ρ and ω are discarded, as discussed above. Instead, we consider vector meson $\phi(1020)$ of $J^{PC} = 1^{--}$ to assign the role generally expected from the vector meson exchanges in the $K^\pm N \rightarrow K^\pm N$ process. Of the parity and C -parity all even, the scalar mesons $f_0(980)$,

$a_0(980)$ and tensor mesons $f_2(1270)$, $a_2(1320)$ decaying to $K\bar{K}$ are included. For the Pomeron exchange we utilize the amplitude in Ref. [15] to describe the reaction cross sections in the momentum region $P_{\text{Lab}} = 100 - 200$, GeV/c. Therefore, we write the elastic scattering amplitudes as,

$$\mathcal{M}(K^\pm p) = f_0 + a_0 \mp \phi + f_2 + a_2 + \mathbb{P}, \quad (8)$$

$$\mathcal{M}(K^\pm n) = f_0 - a_0 \mp \phi + f_2 - a_2 + \mathbb{P}, \quad (9)$$

where the ϕ meson of C -parity odd changes sign between K^+ and K^- projectiles and the isovector mesons a_0 and a_2 change signs between proton and neutron targets by isospin symmetry.

From the isospin relations between the above amplitudes,

$$\begin{aligned} \mathcal{M}(K^+n \rightarrow K^0p) \\ = \mathcal{M}(K^+p \rightarrow K^+p) - \mathcal{M}(K^+n \rightarrow K^+n), \end{aligned} \quad (10)$$

$$\begin{aligned} \mathcal{M}(K^-p \rightarrow \bar{K}^0n) \\ = \mathcal{M}(K^-p \rightarrow K^-p) - \mathcal{M}(K^-n \rightarrow K^-n), \end{aligned} \quad (11)$$

the charge exchange amplitudes are given by

$$\mathcal{M}(K^+n \rightarrow K^0p) = \mathcal{M}(K^-p \rightarrow \bar{K}^0n) = 2(a_0 + a_2) \quad (12)$$

Given the Reggeized amplitudes relevant to scalar, vector, and tensor meson exchanges in Ref. [15], we now discuss the determination of coupling constants of the meson exchange in the t -channel.

- Scalar meson exchange

Scalar mesons are expected to give contributions in the low momentum region. As to scalar meson-nucleon coupling constants, we appreciate that f_0NN and a_0NN are still hypothetical yet. From the $q\bar{q}$ structure of the scalar meson the QCD-inspired model such as QCD sum rules predicts that $g_{f_0NN} = 0$ and $g_{a_0NN} = 12$, whereas these are $g_{f_0NN} = 10.3$ and $g_{a_0NN} = -8.5$ in the case of the four quark state $q^2\bar{q}^2$ structure [16]. On the other hand, in the vector meson photoproduction, $\gamma p \rightarrow \phi p$, the scalar meson nonet is considered with the mixing angle θ_s between the singlet and octet members to write the $SU_f(3)$ relations among a_0 , f_0 and σ mesons as [17]

$$g_{a_0NN} = \frac{F + D}{3F - D} \frac{1}{\cos \theta_s} g_{\sigma NN}, \quad (13)$$

$$g_{f_0NN} = -\tan \theta_s g_{\sigma NN}. \quad (14)$$

Given the mixing angle $\theta_s = -3.21^\circ$, and $F/D = 0.575 \pm 0.016$ we obtain $g_{a_0NN} = 31.77 \pm 1.66$ and $g_{f_0NN} = 0.82$ from $g_{\sigma NN} = 14.6$ [18]. Therefore, within the uncertainty in the choice of $g_{\sigma NN}$ the coupling constant g_{a_0NN} is in the range $8.5 - 32$, regardless its sign. We choose $g_{a_0NN} = 15.5$ which is better to describe KN ($\bar{K}N$) charge exchange reactions, and $g_{f_0NN} \approx 0$ which is consistent with QCD sum rule and vector meson photoproduction as well.

The reggeized amplitude for the scalar meson (S) exchange employs the derivative coupling of the scalar meson to $K\bar{K}$ with the coupling vertex [15],

$$\Gamma_{SKK}(q, k) = \frac{g_{SKK}}{m_K} q \cdot k. \quad (15)$$

As the full width of scalar meson a_0 is in a broader range $\Gamma(a_0) = 50-100$ MeV, and no precise measurement of the partial decay width $\Gamma(a_0 \rightarrow K\bar{K})$ is available yet, we have to estimate the partial width from PDG; $\Gamma(a_0 \rightarrow K\bar{K}) = 6.4 - 12.8$ MeV from the ratio $\Gamma(a_0 \rightarrow K\bar{K})/\Gamma(a_0 \rightarrow \eta\pi) = 0.183 \pm 0.024$ with $\Gamma(a_0 \rightarrow \eta\pi) = 35 - 70$ MeV, which is obtained by $\Gamma(a_0 \rightarrow \eta\pi)\Gamma(a_0 \rightarrow \gamma\gamma)/\Gamma(a_0) = 0.21^{+0.08}_{-0.04}$ keV and $\Gamma(a_0 \rightarrow \gamma\gamma) = 0.3 \pm 0.1$ keV. By isospin invariance of two decay channels K^+K^- and $K^0\bar{K}^0$ we further consider the factor of 1/2 for the above width to get $\Gamma(a_0 \rightarrow K^+K^-) = 3.2 - 6.4$ MeV. However, because the scalar meson mass is proximity to the threshold of $K\bar{K}$ decay, the estimate of coupling constant is highly sensitive to what mass is chosen for the $K\bar{K}$ threshold. From the decay width for the derivative coupling SKK vertex,

$$\Gamma(S \rightarrow K^+K^-) = \frac{g_{SKK}^2 k (E_K^2 + k^2)^2}{8\pi m_S^2 m_K^2}, \quad (16)$$

where k is three-momentum of the decaying meson in the c.m. frame and E_K is its energy, we determine $g_{a_0KK} = \pm 5.33$ with the threshold mass $m_{a_0} = 988$ MeV and $\Gamma(a_0 \rightarrow K^+K^-) = 5.06$ MeV taken, though we use $m_{a_0} = 980$ MeV in the analysis of the reaction process.

- Vector meson exchange

The decay width $\phi \rightarrow K^+K^-$ is given by

$$\Gamma(\phi \rightarrow K^+K^-) = \frac{g_{\phi KK}^2 k^3}{6\pi m_\phi^2}, \quad (17)$$

and the decay width $\Gamma(\phi \rightarrow K^+K^-) = 2.1$ MeV taken from PDG yields $g_{\phi KK} = \pm 4.46$. In ϕ vector meson photoproduction [17, 19] the tensor coupling constant $g_{\phi NN}^t \approx 0$ could obtain a consensus. However, the vector coupling constant $g_{\phi NN}^v$ is controversial; the value $g_{\phi NN}^v = -0.24$ was used in Ref. [17] which is consistent with $g_{\phi NN} = -0.25$ by the strict OZI rule [20]. Meanwhile, the analysis of NN and YN scattering yields $g_{\phi NN} = \pm 1.12$ [21], and ± 3.47 [22], confirming evidence for OZI evading process at the ϕNN vertex. From the universality of ϕ vector meson dominance, we here take $g_{\phi NN}^v = -3.0$, as a trial, which is close to $g_{\phi KK}$ with $g_{\phi NN}^t = 0$ for the ϕNN coupling vertex. We note that whatever values it could take among those suggested in literature, its contribution should be insignificant in comparison to f_2 and a_2 , because of the lower lying trajectory as shown in Table I.

- Tensor meson exchange

The exchange of tensor meson includes isoscalar f_2 meson with the decay width $\Gamma(f_2 \rightarrow K\bar{K}) = 4.29$ MeV

TABLE I. Physical constants and Regge trajectories with the corresponding phase factors for $K^\pm N \rightarrow K^\pm N$. The symbol φ stands for a_0 , ϕ , f_2 and a_2 . The meson-baryon coupling constants for vector meson and tensor meson are denoted by g_{VNN}^v (g_{VNN}^t), and $g_{TNN}^{(1)}$ ($g_{TNN}^{(2)}$), respectively.

Meson	Trajectory(α_φ)	Phase factor	$g_{\varphi KK}$	$g_{\varphi NN}$
a_0	$0.7(t - m_{a_0}^2)$	$(1 + e^{-i\pi\alpha_{a_0}})/2$	5.33	15.5
ϕ	$0.9t + 0.1$	$(-1 + e^{-i\pi\alpha_\phi})/2$	4.46	-3.0 (0)
f_2	$0.9t + 0.53$	$(1 + e^{-i\pi\alpha_{f_2}})/2$	3.53	6.45 (0)
a_2	$0.9t + 0.43$	$(1 + e^{-i\pi\alpha_{a_2}})/2$	-2.45	1.4 (0)

which is estimated from the full width 186.7 MeV with the fraction 4.6%. In the isovector channel the a_2 meson is considered with the decay width $\Gamma(a_2 \rightarrow K\bar{K}) = 2.69$ MeV from the full width 109.8 MeV and the fraction 4.9%. The factor of 1/2 is taken into account in both decay widths by the same reason as in the case of scalar meson.

By using the decay width for the tensor meson (T) coupling to $K\bar{K}$,

$$\Gamma(T \rightarrow K^+K^-) = \frac{4g_{TKK}^2 k^5}{15\pi m_T^4}, \quad (18)$$

we estimate the coupling constants as $g_{f_2KK} = \pm 3.53$ and $g_{a_2KK} = \pm 2.45$ from the respective decay widths given above.

To keep consistency with the coupling constants of $f_2 NN$ in the πN scattering [15] we resume $g_{f_2 NN}^{(1)} = 6.45$ and $g_{f_2 NN}^{(2)} = 0$, the latter of which is rather stringent in order to agree with πN polarization observables. The determination of $a_2 NN$ coupling is discussed in photoproduction of charged kaon [23], where the $SU(3)_f$ symmetry dictates $g_{a_2 NN}^{(1)} = 1.4$ and $g_{a_2 NN}^{(2)} = 0$ to agree with experimental data. We keep these values in the present calculation.

A canonical form of the trajectory $\alpha_\varphi(t) = \alpha'_\varphi(t - m_\varphi^2) + J$ is considered for the φ Regge-pole of spin- J . The slopes of f_2 and a_2 are taken to be the same with those of exchange degenerate pair ω and ρ , respectively [15]. Nevertheless, the phases of f_2 and a_2 Regge poles are taken to be exchange nondegenerate for the elastic process, because of the absence of ω and ρ from the present calculation. The slope of a_0 trajectory is assumed to be the same with that of scalar meson σ [15] as a member of the scalar meson nonet. The trajectory of ϕ is taken from Ref. [24]. A summary of physical constants is listed in Table I including the coupling constants and trajectories with the corresponding phase factors.

- Pomeron exchange

In Ref. [15] for $\pi^\pm p$ elastic scatterings we constructed the Pomeron exchange arising from the quark-Pomeron coupling picture.

With the Pomeron trajectory,

$$\alpha_{\mathbb{P}}(t) = 0.12t + 1.06, \quad (19)$$

and the quark-pion coupling strength $f_{\pi qq}$ from the Goldberger-Treiman relation at the quark level, the cross sections for $\pi^\pm N$ elastic scattering up to $P_{\text{Lab}} = 250$ GeV/c were reproduced by a single exchange of Pomeron. It is straightforward to apply the formulation of the Pomeron in Ref. [15] to $K^\pm p$ elastic scattering¹ with minor changes, e.g., the quark-kaon coupling constant f_{Kqq} , the quark-Pomeron coupling strength β_s with the strange quark mass m_q , instead of those for pion and d quark.

In numerical calculations we take $\beta_u = 2.07$ and $\beta_s = 1.6$ GeV⁻¹, as before [18], and $m_q = 500$ MeV in favor of the strange quark involved. Let us now determine the coupling strength f_{Kqq} . Unlike the case of $f_{\pi qq}$, however, the Goldberger-Treiman relation from the SU(3) symmetry is not likely to give the reliable answer by the large symmetry breaking. From the phenomenological point of view the ratio of elastic cross sections for K^+p and π^+p at high momenta could be a hint to a determination of f_{Kqq} [25]. At $P_{\text{Lab}} = 250$ GeV/c where there exists only the Pomeron exchange and all others are assumed to be minimal, the ratio of cross sections from world data gives

$$\frac{\sigma_{el}(K^+p)}{\sigma_{el}(\pi^+p)} \approx 0.836, \quad (20)$$

and, hence,

$$\frac{|\mathcal{M}_{el}(K^+p)|}{|\mathcal{M}_{el}(\pi^+p)|} \approx \frac{f_{Kqq}^2 m_K^2 \beta_s}{f_{\pi qq}^2 m_\pi^2 \beta_d} \approx \sqrt{0.836}, \quad (21)$$

which yields $f_{Kqq} = 0.82$ by taking $f_{\pi qq} = 2.65$ [15]. This means that, in order to obtain a better agreement with the high momentum $K^\pm p$ data, we may well treat the quark-meson coupling constant f_{Kqq} rather as a parameter around the value above in the fitting procedure to cross section data.

A. $K^\pm p \rightarrow K^\pm p$

Figure 1 shows the differential cross sections selected in the same momentum range to compare K^+p with K^-p elastic scattering. Since the data at $P_{\text{Lab}} = 100$ and 200 GeV/c are governed by a pure Pomeron exchange we exploit them to determine the quark-Pomeron coupling strength, and obtain $f_{Kqq} = 0.988$ with the trajectory in

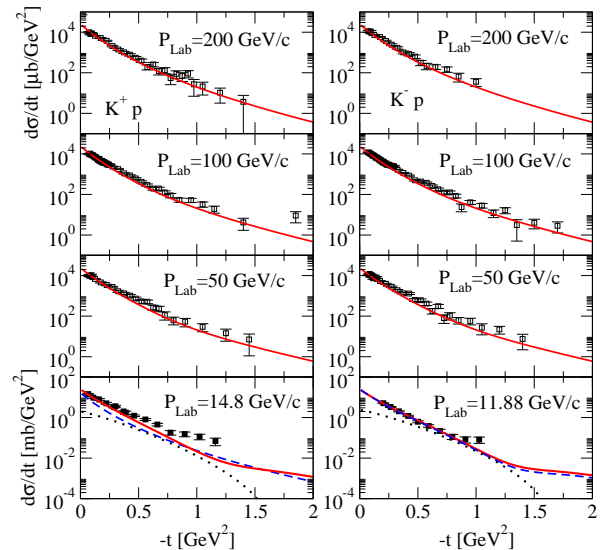


FIG. 1. Differential cross sections for elastic K^+p (left column) and K^-p (right column). Cross sections at $P_{\text{Lab}} = 100$ and 200 GeV/c are featured by Pomeron exchange. Data at $P_{\text{Lab}} = 50, 100,$ and 200 GeV/c for both reactions are taken from Ref. [26]. Data at $P_{\text{Lab}} = 14.8$ GeV/c for K^+p and 11.88 GeV/c for K^-p are from Ref. [27].

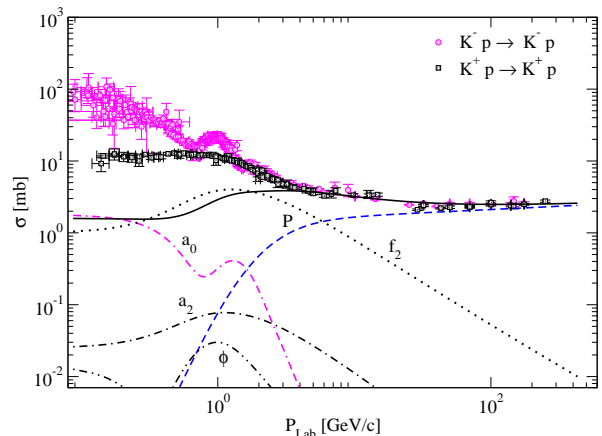


FIG. 2. Total elastic cross sections for $K^+p \rightarrow K^+p$ and $K^-p \rightarrow K^-p$. The solid curve for the total cross section results from the full calculation of $K^+p \rightarrow K^+p$. The difference between cross sections of K^+p and K^-p is negligible by the ϕ contribution of the order of 10^{-2} . Data are taken from PDG.

Eq. (19), while the cutoff parameter $\mu = 2.5$ GeV and $n = 1$ are fixed for the kaon form factor [15],

$$F_K(t, W) = (1 - t/\Lambda^2)^{-n} \quad (22)$$

and $\Lambda(W) = \frac{k}{\mu}(W - W_{th})$. In a good agreement with all the data selected, we regard $f_{Kqq} = 0.988$ to be reasonable because it is close to 0.82 from the ratio in Eq. (21). The dominance of the Pomeron exchange followed by the tensor meson f_2 is shown in the lowest panels. Contributions of f_2 (dotted) and Pomeron (dashed) are

¹ There is the Pomeron coupling to strange quark in the KN reaction in addition to $u(d)$ quark in the quark loop integral [15]. Nevertheless, such a difference between the two couplings by mass difference is neglected for simplicity, as the quark masses between strangeness and up(down) quarks are not widely different in the constituent quarks we adopted here.

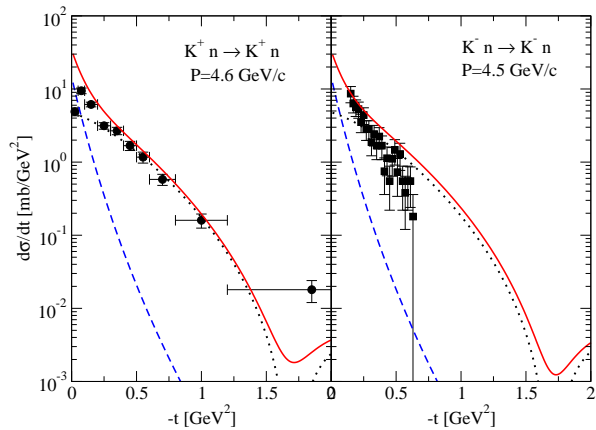


FIG. 3. Differential cross sections for $K^+n \rightarrow K^+n$ at $P_{\text{Lab}} = 4.6$ GeV/c and $K^-n \rightarrow K^-n$ at $P_{\text{Lab}} = 4.5$ GeV/c, respectively. Notations for the curves are the same as in Fig. 2. Data are taken from Refs. [30] and [32], respectively.

shown at $P_{\text{Lab}} = 14.8$ for K^+p and 11.88 GeV/c for K^-p reactions, respectively.

In Fig. 2 we present total cross sections for K^+p and K^-p elastic processes where an agreement with data at high momenta $P_{\text{Lab}} \approx 3$ GeV/c is obtained by the exchanges of f_2 and Pomeron. Without a fitting procedure for hadron coupling constants we describe elastic scattering over the region $P_{\text{Lab}} \approx 3$ GeV/c up to 250 GeV/c. As discussed above, the distinction between the two reactions disappears at high momenta, because of the small contribution of ϕ . It is worth observing the similarity between $\pi^\pm N$ [15] and $K^\pm N$ total elastic cross sections where the roles of σ , ρ and ω in the former reactions are replaced by those of a_0 , a_2 and ϕ of the same order of magnitude, respectively. Also, the $K^\pm p$ elastic scatterings are dominated by the tensor meson f_2 at intermediate and the Pomeron exchange at high momenta to exhibit the isoscalar nature of the reactions.

Below $P_{\text{Lab}} \approx 3$ GeV/c the large discrepancy between the t -channel Regge predictions and data could presumably be resolved by considering nuclear interaction for K^+p [28], and the $\bar{K}N$ coupled states for the K^-p elastic scatterings, respectively [5].

B. $K^\pm n \rightarrow K^\pm n$

Experimental data on neutron targets are extracted from kaon scattering off deuteron, in which case proton is assumed to be a spectator. Data at high momenta are rare and contain some uncertainties due to the procedures such as impulse approximation, Glauber screening, and Fermi motion taken usually in the analysis of deuteron data. A few data points on the total cross section for K^+n elastic reaction are found at $P_{\text{Lab}} = 2.97$ GeV/c [29] and 4.6 GeV/c [30], respectively. For the K^-n reaction the total cross section data are reported at $P_{\text{Lab}} = 2.2$ GeV/c [31] and 4.5 GeV/c [32], respec-

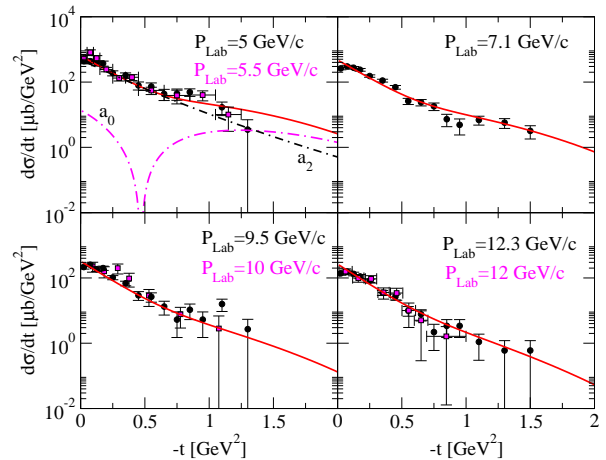


FIG. 4. Differential cross sections for $K^-p \rightarrow \bar{K}^0n$ and $K^+n \rightarrow K^0p$. Solid curves for cross sections are calculated at $P_{\text{Lab}} = 5.5, 7.1, 10,$ and 12 GeV/c by using the $K^+p \rightarrow K^0n$ amplitude, which shares with the $K^-p \rightarrow \bar{K}^0n$ amplitude in common. The respective contributions of $a_0(980)$ and $a_2(1320)$ are shown in the upper left panel. Data of $K^-p \rightarrow \bar{K}^0n$ (black circles) are taken from Ref. [33]. Data of $K^+n \rightarrow K^0p$ (magenta squares) at $P_{\text{Lab}} = 5.5, 10,$ and 12 GeV/c are taken from Refs. [34][35][36].

tively. Therefore, no data are enough to analyze high momentum behavior of the reactions. Similar to $K^\pm p$ elastic processes, however, we expect that the difference between K^+n and K^-n elastic reactions is negligible due to the mentioned role of vector meson ϕ . Furthermore, as the $a_0 + a_2$ exchanges in the elastic $K^\pm n$ reaction play the role opposite to the $K^\pm p$ from Eqs. (8) and (9), the difference between them could be less apparent, and the total elastic cross sections for $K^\pm n$ at high momentum are to be the same as those of $K^\pm p$ with the same role of the isoscalar exchanges f_2 and Pomeron. We present differential cross sections for K^+n at $P_{\text{Lab}} = 4.6$ GeV/c and K^-n at 4.5 GeV/c in Fig. 3. We use the kaon form factor with $\mu = 2.5$ GeV and $n = 3$ for the Pomeron exchange in Eq. (22) for $K^\pm n$ elastic reactions. An overall agreement with differential cross sections is predicted, though the discrepancy with K^+n data in the large $-t$ is shown due to the dominance of f_2 exchange with the exchange nondegenerate phase over the Pomeron contribution in these intermediate momenta, 4.5 and 4.6 GeV/c.

III. CHARGE EXCHANGE SCATTERING

A. $K^+n \rightarrow K^0p$ and $K^-p \rightarrow \bar{K}^0n$

Charge exchange K^+n and K^-p are good places to examine the validity of simple $a_0 + a_2$ exchanges. A collection of data on these reactions exhibits the same dependence of both cross sections upon energy and an-

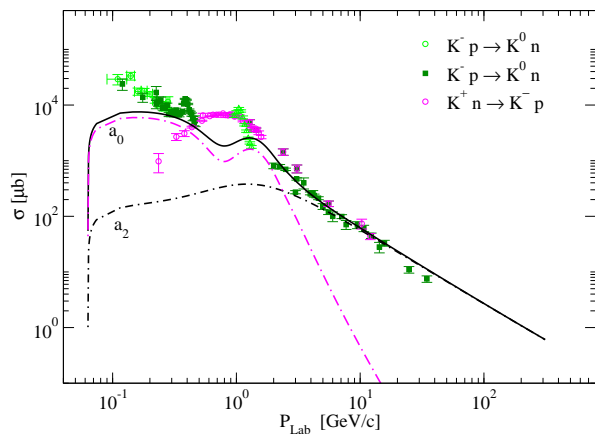


FIG. 5. Total charge exchange cross sections for $K^-p \rightarrow \bar{K}^0 n$ and $K^+n \rightarrow K^0 p$. The solid cross section is presented for the $K^+n \rightarrow K^0 p$ process. The contribution of the a_2 exchange agrees with data at high momenta. Data of $K^+n \rightarrow K^0 p$ are taken from Refs. [35, 37]. Data of $K^-p \rightarrow \bar{K}^0 n$ are from Refs. [30, 33, 38–41].

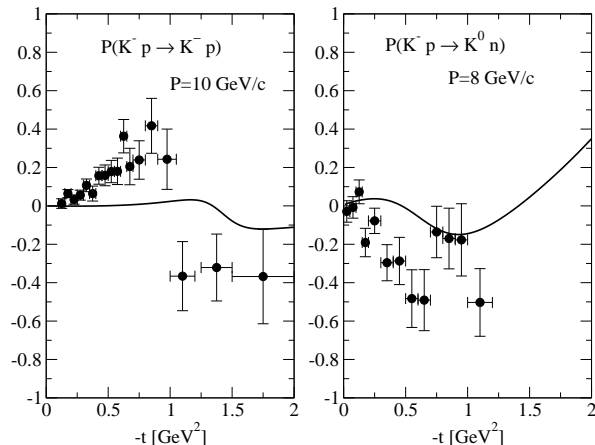


FIG. 6. Polarization P of $K^-p \rightarrow K^-p$ at $P_{\text{Lab}} = 10 \text{ GeV}/c$ and $K^-p \rightarrow \bar{K}^0 n$ at $P_{\text{Lab}} = 8 \text{ GeV}/c$. Data are taken from Refs. [42, 43].

gles at high momenta, as shown in Figs. 4 and 5. The differential cross sections for both reactions in the same momentum range are presented in Fig. 4. We obtain a fair agreement with data by using the coupling constants and the exchange nondegenerate phase for a_0 chosen in Table I for the combined analysis. However, in these reactions, the complex phase, $\text{EXP}[-i\pi\alpha_{a_2}(t)]$ for the a_2 exchange is favored in order to agree with cross section data rather than the exchange nondegenerate phase. In Fig. 5 such an expected behavior from the a_2 exchange with the complex phase is clear in the total cross section, where the cross section over $P_{\text{Lab}} \approx 4 \text{ GeV}/c$ should be reproduced only by the a_2 exchange. Meanwhile, the a_0 exchange is found to play a leading role in the low momentum region. Throughout the successful description

of reaction cross sections as presented in Figs. 4 and 5, it could be concluded that the isospin symmetry is valid between all six channels as stated in Eqs. (10) and (11).

Finally, we discuss polarization (P) of KN ($\bar{K}N$) scattering. It is observed via the interference between the spin-nonflip and spin-flip amplitudes of exchanged mesons [15]. Therefore, we simply figure out vanishing of polarization at high momenta, because there contributes only Pomeron exchange. Within the present framework the predictions for polarization data at intermediate momenta are poor, as shown by the case of K^-p elastic reaction in Fig. 6. Nevertheless, due to the interference between a_0 with the exchange nondegenerate phase and a_2 with the complex phase the polarization of $K^-p \rightarrow \bar{K}^0 n$ at $P_{\text{Lab}} = 8 \text{ GeV}/c^2$ is reproduced to some degree. The polarizations in both reactions follow the behavior of data along with t -dependence in Fig. 6. Inclusion of the cut is likely to reinforce the strength of the polarization to agree with data, as demonstrated in Ref. [15].

IV. SUMMARY AND DISCUSSION

We have performed a combined analysis of KN and $\bar{K}N$ scatterings with a set of coupling constants common in four elastic and two charge exchange processes in the Regge realm. The scattering amplitude is obtained by reggeizing the relativistic Born amplitude for the t -channel meson exchange with the decay width to $K\bar{K}$ allowed kinematically and listed in the PDG. Thus, the exchanges of ρ and ω are excluded from the present framework and the present approach needs none of the hadron form factors for such off-shell meson exchanges. This is the most distinctive feature from previous calculations at high momenta, though contradicting to existing model descriptions.

Within the present approach the isoscalar f_2 and Pomeron exchanges are found to be dominant in four elastic channels, while the charge exchange processes exhibit the isovector nature via the simple a_0 and a_2 exchanges. The exchange of the soft Pomeron which is constructed on the basis of the quark-Pomeron coupling picture reproduces the diffraction feature of elastic cross sections to a good degree. Nevertheless, in order for the present analysis to be valid for the threshold region, inclusion of partial wave contributions is necessary to describe the reaction mechanisms induced by either the propagation of exotic channels in K^+N reactions, or the meson-baryon couplings in the $\bar{K}N$ channels. This should be a subject of future study to make complete our understanding of KN ($\bar{K}N$) scattering based on the t -channel exchange discussed here as a background contribution. Work on this direction is ongoing and the results will appear elsewhere.

ACKNOWLEDGMENTS

This work was supported by the National Research Foundation of Korea Grant No. NRF-2017R1A2B4010117.

Appendix A: Conventional Approach versus the Reggeized model

It has been a long standing idea that the ρ and ω vector meson exchanges are included to account for the difference between K^+p and K^-p total cross sections at high momenta. [7]. At this point, the elastic cross section should not be confused with the total (reaction) cross section. The former reaction cross sections are observed to coincide to each other at high momenta, which is understandable only by the isoscalar Pomeron exchange.

For illustration purpose, we make a simulation of $\rho + \omega$ exchanges, despite the decay mode neither $\rho \rightarrow K\bar{K}$ nor $\omega \rightarrow K\bar{K}$ is allowed. These vector mesons could be considered in the elastic $K^\pm N$ scattering by substituting $f_2 \rightarrow (f_2 \mp \omega)$ and $a_2 \rightarrow (a_2 \mp \rho)$ in Eqs. (8) and (9) [10] with the exchange degenerate phase ($a_2 \mp \rho$) = 1, or $e^{-i\pi\alpha(t)}$ for the minus, or plus sign. The trajectories $\alpha_\rho(t) = 0.9t + 0.46$ and $\alpha_\omega(t) = 0.9t + 0.44$ are used. To be consistent with other meson exchanges we avoid

employing cutoff form factors in the meson baryon coupling vertices. However, given the coupling constants $g_{\rho KK} = g_{\rho NN}^v$, and $g_{\omega KK} = g_{\omega NN}^v$, which we usually take 2.6 and 15.6, respectively, from vector meson dominance [12, 14] the inclusion of $\rho + \omega$ exchanges lead to a complete failure in reproducing elastic data. Figure 7 shows inconsistency of model predictions for the $K^\pm p$ elastic cross sections, even if we use such unnatural values $g_{\rho KK} = 0.1$ and $g_{\omega KK} = -0.1$, while the vector-meson nucleon coupling constants remain unchanged.

As demonstrated by the solid curve for reference, the coincidence of $K^\pm p$ cross sections at high momenta can be achieved only from the absence of $\rho + \omega$ exchanges either or they should be negligible at least within the present approach. To investigate the possibility of spin-1 vector meson further, we test the contribution of $\rho'(1450)$ exchange with the trajectory $\alpha_{\rho'} = t - 1.23$. As the coupling constants are still evasive, we deduced $G_{\rho'}^v \approx 10$ and $G_{\rho'}^t \approx -20$ from those values, 40 and -75 , which are corresponding to the πN case [15]. Assuming the universality, $g_{\rho'\pi\pi} = g_{\rho'NN}^v \approx 6.32$, and we take half the value of it for the present case with $g_{\rho'KK} = g_{\rho'NN}^v$ by the same reason. From the ratio of vector to tensor coupling, $\kappa_{\rho'\pi\pi} \approx -1.88$ is deduced. The result hardly alters the cross section in the momentum region of our interest. These findings show that they are inadequate for the present framework which is based on nearly on-shell Born amplitude for the reggeization of t -channel meson exchange.

-
- [1] R. A. Arndt, I. I. Strakovsky and R. L. Workman, Nucl. Phys. A **754**, 261c (2005).
- [2] Ya. I. Azimov, R. A. Arndt, I. I. Strakovsky, R. L. Workman, and K. Goeke, Eur. Phys. J. A. **26**, 79 (2005).
- [3] J. S. Hyslop, R. A. Arndt, L. D. Roper, and R. L. Workman, Phys. Rev. D **46**, 961 (1992).
- [4] G. Giacomelli, P. Lugaesi-Serra, G. Mandrioli, A. Minguzzi-Ranzi, A. M. Rossi, F. Griffiths, A. A. Hirata, R. Jennings, B. C. Wilson, G. Ciapetti, P. Guidoni, G. Mastrantonio, A. Nappi, D. Zanello, G. Alberi, E. Castelli, P. Poropat, M.Sessa (BGRT Collaboration), Nucl. Phys. B **56**, 346 (1973).
- [5] K. Aoki and D. Jido, Prog. Theor. Exp. Phys. **2017**, 103D01 (2017).
- [6] Y. Ikeda, T. Hyodo, W. Weise, Phys. Lett. B **706** 63 (2011).
- [7] A. Donnachie and P. V. Landshoff, Phys. Lett. B **296** 227 (1992).
- [8] E. Oset and A. Ramos, Nucl. Phys. A **635** 99 (1998).
- [9] A. C. Irving and R. P. Worden, Phys. Rept. **34** 117 (1977).
- [10] R. J. N. Phillips and W. Rarita, Phys. Rev. **139**, B1336 (1965).
- [11] W. Rarita and B. M. Schwamschild, Phys. Rev. **162**, 1378 (1967).
- [12] R. Büttgen, K. Holinde, and J. Speth, Phys. Lett. B **163**, 305 (1985).
- [13] J. Nys, A. N. Hiller Blin, V. Mathieu, C. Fernández-Ramírez, A. Jackura, A. Pilloni, J. Ryckebusch, A. P. Szczepaniak, G. Fox, Phys. Rev. D **98**, 034020 (2018).
- [14] F.-Q. Wu and B.-S. Zou, arXiv:0710.5855[hep-ph], Chinese Phys. C (HEP & NP) **32**, 629 (2008).
- [15] K.-J. Kong and B.-G. Yu, Phys. Rev. C **98**, 045207 (2018).
- [16] G. Erkol, M. Oka, Th. A. Rijken, and R. G. E. Timmermans, Phys. Rev. C **73**, 044009 (2006).
- [17] A. I. Titov, T.-S. H Lee, H. Toki,1, and O. Streltsova, Phys. Rev. C **60**, 035205 (1999).
- [18] B.-G. Yu and K.-J. Kong, Phys. Rev. D **95**, 014020 (2017).
- [19] Y. Oh, J. Kor. Phys. Soc. **43**, S20 (2003).
- [20] U.-G. Meißner, V. Mull, J. Speth, and J. W. Van Orden, Phys. Lett. B **408**, 381 (1997).
- [21] M. M. Nagels T. A. Rijken, and J. J. de Swart, Phys. Rev. D **17**, 768 (1978).
- [22] M. M. Nagels T. A. Rijken, and J. J. de Swart, Phys. Rev. D **20**, 1633 (1979).
- [23] B.-G. Yu and T. K. Choi, and W. Kim, Phys. Lett. B **701**, 332 (2011).
- [24] P. D. B.Collins, *An Introduction to Regge Theory & High Energy Physics* Cambridge University Press (1977).
- [25] A. A. Godizov, Eur. Phys. J. C **76**, 361 (2016).
- [26] C. W. Akerlof, R. Kotthaus, R. L. Loveless, D. I. Meyer, I. Ambats, W. T. Meyer, C. E. W. Ward, D. P. Eartly, R. A. Lundy, S. M. Pruss, D. D. Yovanovitch, and D. R. Rust, Phys. Rev. D **14**, 2864 (1976).

- [27] K. J. Foley *et al.*, Phys. Rev. Lett. **11**, 503 (1963); *ibid.* **15**, 45 (1965).
 [28] B. R. Martin, Nucl. Phys. B **94**, 413 (1975).
 [29] K. Buchner, Nucl. Phys. B **44**, 110 (1972).
 [30] G. Dehm *et al.*, Nucl. Phys. B **60**, 493 (1973).
 [31] Y. Declais, J. Duchon, M. Louvel, J.-P. Patry, J. Seguinot, P. Baillon, C. Bricman, M. Ferro-Luzzi, J.-M. Perreau, T. Ypsilantis, CERN-77-16. hep-database <http://durpdg.dur.ac.uk/view/ins121681/last>.
 [32] C. Declercq, D. Johnson, J. Lemonne, P. Peeters, P. Renton, P. Van Binst, G. Vanhomwegen, and J. Wickens, Nucl. Phys. B **126**, 397 (1977).
 [33] P. Astbury *et al.*, Phys. Lett B **23**, 396 (1966).
 [34] D. Cline, J. Penn and D. D. Reeder, Nucl. Phys. B **22**, 247 (1970).
 [35] M. Haguenaer *et al.*, Phys. Lett B **37**, 538 (1971).
 [36] A. Firestone, G. Goldhaber, A. Hirata, D. Lissauer, and G. H. Trilling, Phys. Rev. Lett. **25**, 958 (1970).
 [37] C. J. S. Damerell *et al.*, Nucl. Phys. B **94**, 374 (1975).
 [38] T. S. Mast, M. Alston-Garnjost, R. O. Bangerter, A. S. Barbaro-Galtieri, F. T. Solmitz, and R. D. Tripp, Phys. Rev. D **14**, 13 (1976).
 [39] G. S. Abrams and B. Sechi-Zorn, Phys. Rev. **139**, B454 (1965).
 [40] K. J. Foley *et al.*, Phys. Rev. D **9**, 42 (1974).
 [41] B. Conforto *et al.*, Nucl. Phys. B **105**, 189 (1976).
 [42] M. Borghini *et al.*, Phys. Lett. B **36**, 497 (1971).

- [43] W. Beusch *et al.*, Phys. Lett. B **46**, 477 (1973).

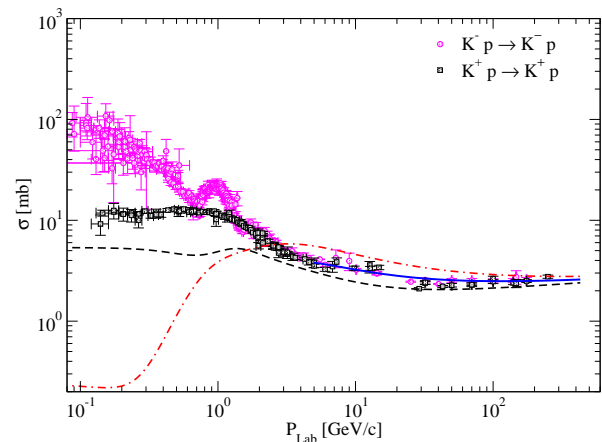


FIG. 7. Effect of $\rho + \omega$ exchanges on the elastic $K^\pm p$ cross sections. The discrepancy between $K^- p$ (upper dash-dotted) and $K^+ p$ (lower dashed) curves at high momenta cannot be reduced to a common datasets for $K^\pm p$ in the presence of $\rho + \omega$ exchanges. The solid curve from Fig. 2 is presented for comparison.